Field theoretical methods in fluid and plasma theory

Third Part : Applications

(of the field theoretical models

for the two-D fluid and plasma)

Florin Spineanu

Association EURATOM-MEdC Romania

Field theory *vs.* the rest of fluid/plasma theory
Results of a comparison

1. the field theoretical model of the current profiles in tokamak is compatible with the Liouville equation. Comparison with the model of Taylor gives interesting suggestions for the physical interpretation of the FT parameters.

2. for the Euler fluid we obtain in FT a possible confirmation of the existence of a current of vorticity leading to concentration into filaments.

3. for the $2D$ plasma in strong magnetic field we obtain patterns of vortical flows that confirm previous calculations.

4. for the LH transtion, we obtain, after a renormalisation of the Larmor radius into an *effective* Larmor radius, profiles of electric fields at the edge (in H mode) that are compatible with the

experiments

5. for the density pinch we are able to build a physical picture that is consistent with the idea that the pinch of density is due to a pinch of vorticity.

6. for the $2D$ atmosphere we obtain quantitative results that compares (very) well with the observations of *tropical cyclone*.

7. for the *Abelian dominance* model the first results show the existence of ring-type vortices.

Two kinds of comparisons: (1)solve the nonlinear equations and compare with experiments; (2)compare the physics behind the classical (e.g. statistical) model and the FT one.

What have-we done until now

Current J Abelian	$\Delta\psi + \exp(\psi) = 0$	statistical	no ρ_s
Euler Non-Abelian	$\Delta\psi + \sinh\psi = 0$	statistical	no ρ_s
Superfluid Abelian	$\Delta\psi = \exp(\psi) - 1$	n.a. (Minardi?)	finite ρ_s
CHM Non-Abelian	$\Delta\psi = \pm\sinh\psi\,(\cosh\psi - 1)$	one and many	finite ρ_s
CHM Abelian	$\Delta\psi = e^{\psi}\left(e^{\psi} - 1\right)$	topological	finite ρ_s

The Liouville equation

Possible model for (1)filament of current on a magnetic surface; (2)for the *snake* of density.

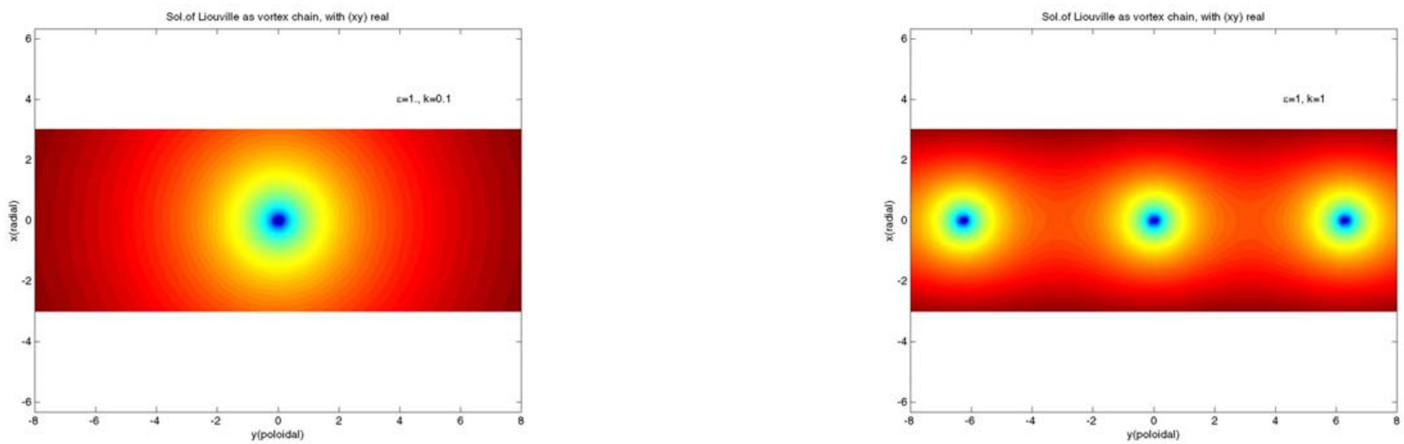

Figure 1: Solution of Kelvin-Stuart type.

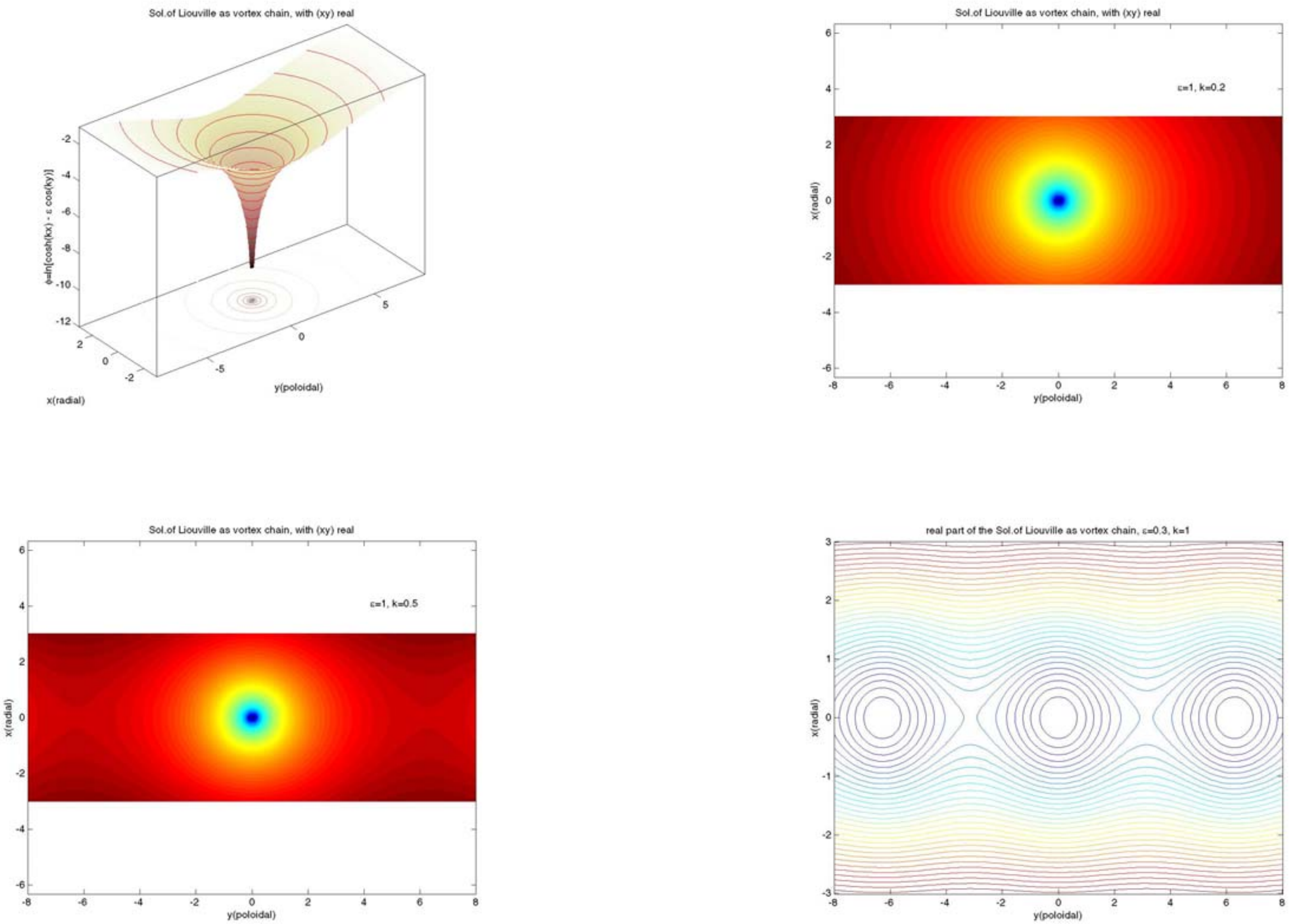

Figure 2: Solution of Kelvin-Stuart type.

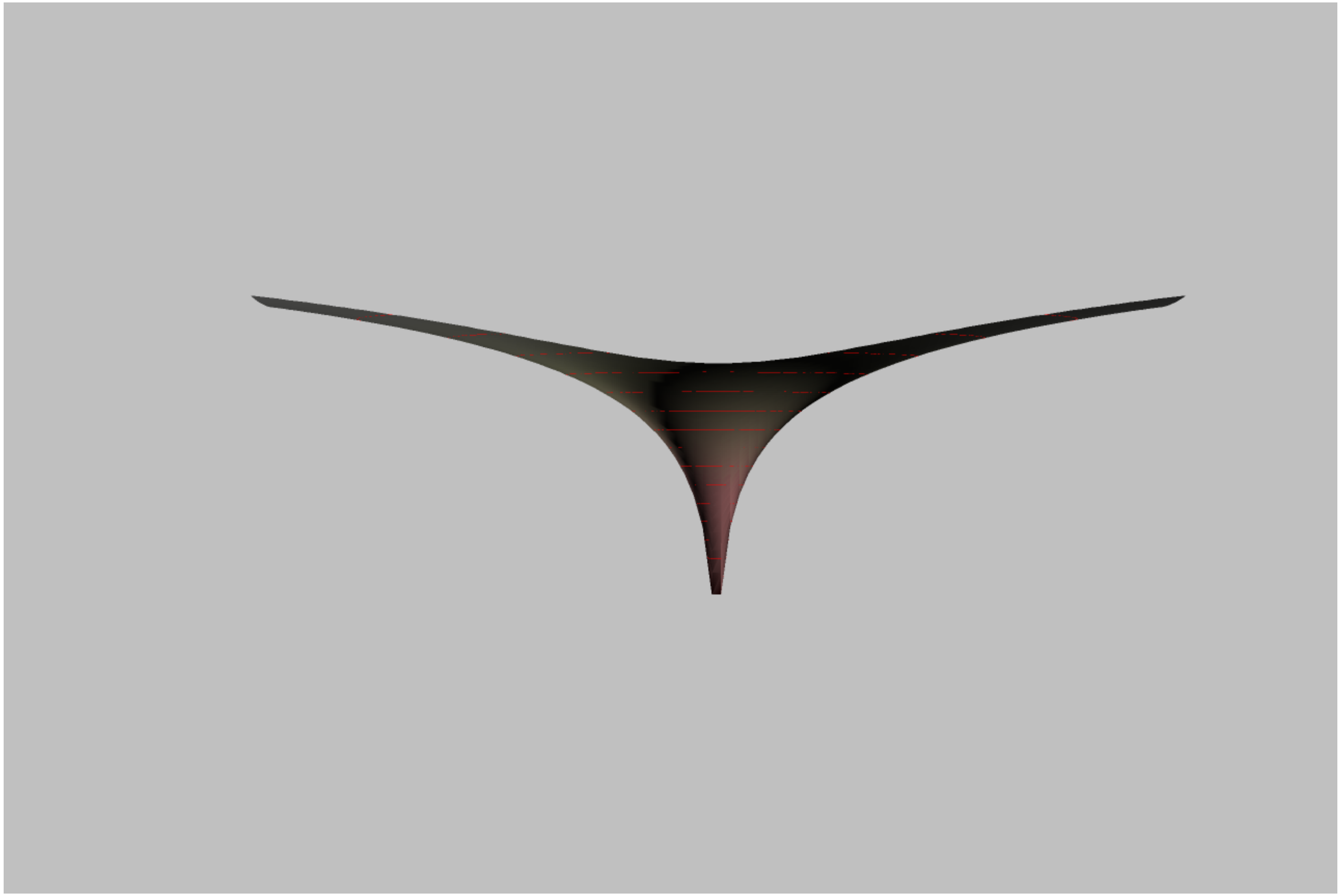

Check if your Acrobat is more than 6 then click and drag

Classical interpretation of natural current profile in tokamak

Current self-organization in tokamak. The equation is

$$\nabla\times\left(\mathbf{J}\times\mathbf{B}\right)=0 \qquad \text{or} \qquad B_0\frac{\partial J}{\partial z}+\left(\mathbf{B}_\perp\cdot\nabla_\perp\right)J=0$$

$$\text{with} \qquad \mathbf{B}_\perp=-\nabla\psi\times\widehat{\mathbf{n}} \qquad \text{and} \qquad J\equiv J_z=\nabla_\perp^2\psi$$

Taylor (1993): the current density consists of *filaments*, acted upon by $\mathbf{B}_\perp$ as a velocity field and with z as time. The position of a filament is $\mathbf{r}_i\left(z\right)\equiv\left[x_i\left(z\right),y_i\left(z\right)\right]$ and the equations of motion are (all filaments are assumed equal j_0)

$$\begin{aligned} j_0\frac{dx_i}{dz} &= \frac{1}{B_0}\frac{\partial H}{\partial y_i} \\ j_0\frac{dy_i}{dz} &= -\frac{1}{B_0}\frac{\partial H}{\partial x_i} \end{aligned}$$

where

$$
\begin{aligned}
H &= \sum_{k<i} j_0^2 U\left(\mathbf{r}_i, \mathbf{r}_k\right) \\
\nabla_\perp^2 U\left(\mathbf{r}, \mathbf{r}^{'}\right) &= \delta\left(\mathbf{r} - \mathbf{r}^{'}\right)
\end{aligned}
$$

In an infinite region, the Green function $U\left(\mathbf{r}, \mathbf{r}^{'}\right)$ of the Laplace operator is

$$
U\left(\mathbf{r}, \mathbf{r}^{'}\right) = \ln\left|\mathbf{r} - \mathbf{r}^{'}\right|
$$

The current distribution and the magnetic flux function ψ (streamfunction)

$$
\begin{aligned}
J &= \sum_i j_0 \delta\left(\mathbf{r} - \mathbf{r}_i\right) \qquad (1) \\
\psi &= j_0 \sum_i U\left(\mathbf{r}, \mathbf{r}_i\right)
\end{aligned}
$$

The statistical description of the system

The energy H is conserved and a *microcanonical* ensemble, where the *joint probability distribution* of the positions of N filaments is

$$\rho\left(\{\mathbf{r}_i\}\right) \sim \delta\left(E - H\left\{\mathbf{r}_i\right\}\right)$$

is appropriate. The entropy

$$S = -k \int d\mathbf{r}\ n\left(\mathbf{r}\right) \ln\left[n\left(\mathbf{r}\right)\right]$$

is a measure of the number of *microscopic configurations* corresponding to a *macroscopic configuration* $n\left(\mathbf{r}\right)$.

Statistical equilibrium is obtained by maximizing S (the entropy) under the constraint of energy conservation and fixed total number of filaments

$$\begin{aligned} E \text{ (fixed)} &= j_0 \int d\mathbf{r} \; n(\mathbf{r}) \, \psi(\mathbf{r}) \\ N \text{ (fixed)} &= \int d\mathbf{r} \; n(\mathbf{r}) \end{aligned}$$

$$\psi(\mathbf{r}) = j_0 \int d\mathbf{r}^{'} \; U\left(\mathbf{r}, \mathbf{r}^{'}\right) n\left(\mathbf{r}^{'}\right)$$

The equilibrium current distribution obtained by extremizing

$$S - \beta E - \gamma N$$

is

$$\begin{aligned} J(\mathbf{r}) &= j_0 \langle n(\mathbf{r}) \rangle \\ &= K \exp\left[-\beta j_0 \psi(\mathbf{r})\right] \end{aligned}$$

Circular symmetry: tokamak of radius a

$$\psi(r) = \frac{2}{\lambda} \ln\left(1 + \alpha \frac{r^2}{a^2}\right)$$

where

$$\alpha = J_0 \lambda \frac{a^2}{8\pi}$$

Introducing the total current I,

$$I = N j_0$$

it is found a relation between the *peaking factor* of the current density, α , and the *inverse temperature* β of the current filaments

$$\beta N j_0^2 = \frac{8\pi\alpha}{1+\alpha}$$

Uniform current (which means that the whole plasma volume is chaotic) is obtained for a magnetic temperature $T_m \equiv 1/\beta$ of

$$\alpha = 0 \text{ or } T_m \rightarrow \infty$$

and it is identified a *critical* magnetic temperature T_m^c where the totality of the current is concentrated into a singular central filament,

$$\alpha \to \infty \text{ or } T_m \to T_m^c \equiv \frac{N j_0^2}{8\pi}$$

Values of the magnetic temperatures between 0 and T_m^c are not accessible.

Hollow current profiles correspond to negative magnetic temperatures. They are only accessible through the infinite value of the magnetic temperature, $T_m \to \infty$, which in terms of profiles means that the current passes first through a state of uniform distribution.

To compare with Field Theory we take the two equations

$$\Delta\psi + \left(\frac{2e^2}{c\left|\kappa\right|}\right)\exp\left(\psi\right) = 0$$

The equation is always the same, whatever is the sign in front of the Chern-Simons term.

In Taylor's theory, we have

$$\nabla_{\perp}^{2}\psi = J_0 \exp\left(-\lambda\psi\right)$$

with

$$\begin{aligned} \lambda &= \frac{8\pi\alpha}{J_0 a^2} \\ \frac{8\pi\alpha}{1+\alpha} &= \frac{1}{T_m} N j_0^2 \end{aligned}$$

or

$$\frac{J_0}{\lambda} = \frac{J_0^2 a^2}{8\pi\alpha} = \frac{2e^2}{c\left|\kappa\right|}$$

Then we can translate the results obtained by Taylor:

1. when the peaking factor α goes to 0, (*i.e.* the magnetic temperature $T_m \to \infty$) the current profile is fully relaxed to a uniform distribution; This corresponds of vanishing κ in the field theory: no Chern-Simons is present.
2. when the peaking factor α goes to ∞, (*i.e.* the magnetic temperature

reaches the *critical* value, $T_m \to T_m^c$) the current is strongly concentrated on the axis. This corresponds to infinite value for κ in the field theory, $|\kappa| \to \infty$: the Chern-Simons term is largely dominating everything else in the Lagrangian.

3. Negative magnetic temperature

$$T_m < 0$$

are obtained in the Taylor's model when

$$\alpha < 0$$

or, the current profile is *hollow*. In field theory this corresponds to a change of sign of κ. But the equation remains the same. The field theory starts with a certain sign of κ, then the Chern-Simons term is suppressed (taking $|\kappa| \to 0$) (leading to uniform solution for $\psi \to -\infty$ everywhere, while $\Delta\psi$ may remain finite). After that the CS term is re-established but with an effect which is opposite to the previous regime.

Everything should be seen as an evolution *on the manifold of SELF-DUAL states, or solutions of the Liouville equation.* The parameter that moves the states on this manifold is κ.

The following quantities have dimension of inverse distance squared

$$\frac{J_0}{\lambda} = \frac{2e^2}{c\,|\kappa|} = \frac{1}{\rho^2}$$

where ρ is a distance. This distance will be the *natural* unit of space-like quantities in the problem. We note that the space unit ρ is proportional with κ. We can say that the passage of the system from a concentrated current profile to a hollow current profile includes a state of strong localisation, where the natural space unit is extremely small, which means that different parts of the system are separated and non-interacting (physically this means chaos and uniform current everywhere).

A basis for the discrete model for the Euler fluid

We must start from the definition of the kinetic energy of a physical fluid

$$
\begin{aligned}
E^{phys} &= \int d^2r \frac{1}{2}\rho_0 v_\theta^2 \\
&= \frac{1}{2}\rho_0 \int d^2r \left|\nabla\psi\right|^2 = \frac{1}{2}\rho_0 \int d^2r \left[\nabla\cdot\left(\psi\nabla\psi\right) - \psi\Delta\psi\right] \\
&= \frac{1}{2}\rho_0 \int dl_{\|} \left[\widehat{\mathbf{n}}_r \cdot \left(\psi\nabla\psi\right)\right] - \frac{1}{2}\rho_0 \int d^2r\psi\Delta\psi \\
&= \frac{1}{2}\rho_0 \int dl_{\|} \left(\psi\frac{d\psi}{d\widehat{n}_r}\right) - \frac{1}{2}\rho_0 \int d^2r\psi\omega
\end{aligned}
$$

For the second term

$$\begin{aligned} \Delta\psi &= \omega \\ \psi &= \Delta^{-1}\omega \\ &= \int d^2r' \ln\left(\left|r-r'\right|\right)\omega\left(r'\right) \end{aligned}$$

then

$$\begin{aligned} E^{phys} &= \int d^2r \frac{1}{2}\rho_0 v_\theta^2 \\ &= -\frac{1}{2}\rho_0 \int d^2r \psi\omega = -\frac{1}{2}\rho_0 \int d^2r \omega\left(r\right) \int d^2r' \ln\left(\left|r-r'\right|\right)\omega\left(r'\right) \end{aligned}$$

$$E^{phys} = -\frac{1}{2}\rho_0 \int d^2r \int d^2r' \omega\left(r\right) \ln\left(\left|r-r'\right|\right)\omega\left(r'\right)$$

Point-like vortices (Montgomery and Joyce, 1974)

The equations :

$$\frac{d\mathbf{x}_i}{dt} = \sum_{j \neq i} \frac{K_i}{2\pi} \widehat{\mathbf{e}}_z \times \frac{\mathbf{x}_i - \mathbf{x}_j}{\left| x_i - x_j \right|^2}$$

where

$$\mathbf{x}_i = (x_i, y_i)$$

The same equations represent the motion of particle guiding centre, if the constants are

$$\mathbf{K}_j = -4\pi \frac{e_j}{l} \frac{\mathbf{B}}{B^2}$$

The system can be put in the Hamiltonian form defining the variables

$$(q_i, p_i) = \left| K_i \right|^2 (x_i, y_i sign K_i)$$

$$H = -\frac{1}{2\pi} \sum_{i<j} K_i K_j \ln \left| \mathbf{x}_{ij} \right|$$

and the equations

$$\begin{aligned} \frac{dq_i}{dt} &= \frac{\partial H}{\partial p_i} \\ \frac{dp_i}{dt} &= -\frac{\partial H}{\partial q_i} \end{aligned}$$

reproduce the equations of motion.

The **total Coulomb interaction energy** is a constant of motion:

$$\mathcal{E} = \sum_{i<j} \varphi_{ij} = -2 \sum_{i<j} \frac{e_i e_j}{l} \ln |\mathbf{x}_{ij}|$$

The current of vorticity in the Euler fluid

The FT current

$$
\begin{aligned}
J^0 &= \left[\Psi^\dagger, \Psi\right] \\
J^i &= -\frac{i}{2}\left(\left[\Psi^\dagger, D_i\Psi\right] - \left[\left(D_i\Psi\right)^\dagger, \Psi\right]\right)
\end{aligned}
$$

We obtain

$$
\begin{aligned}
J^x &= \frac{1}{2}\left[2i(a-a^*)\left(\rho_1+\rho_2\right) - i\frac{\partial}{\partial x}\left(\rho_1-\rho_2\right)\right] H \\
J^y &= \frac{1}{2}\left[2(a+a^*)\left(\rho_1+\rho_2\right) - i\frac{\partial}{\partial y}\left(\rho_1-\rho_2\right)\right] H \\
J^0 &= \left(\rho_1-\rho_2\right) H
\end{aligned}
$$

Can-we see a vorticity pinch here ?

The current at self-duality

$$J^x = -\frac{1}{2}\left[\frac{\partial\psi}{\partial y} - \frac{\partial(2\chi)}{\partial x}\right](\rho_1+\rho_2) - \frac{1}{2}i\frac{\partial}{\partial x}(\rho_1-\rho_2)$$

$$J^y = \frac{1}{2}\left[\frac{\partial\psi}{\partial x} + \frac{\partial(2\chi)}{\partial y}\right](\rho_1+\rho_2) - \frac{1}{2}i\frac{\partial}{\partial y}(\rho_1-\rho_2)$$

We have

$$J_+ = \frac{1}{2}i(\rho_1+\rho_2)\,\partial_+[\psi - (2i\chi)] - \frac{1}{2}i\partial_+(\rho_1-\rho_2)$$

$$J_- = -\frac{1}{2}i(\rho_1+\rho_2)\,\partial_-[\psi + (2i\chi)] - \frac{1}{2}i\partial_-(\rho_1-\rho_2)$$

For circular symmetry,

$$\begin{aligned} J_+ &= (\rho_1+\rho_2)\,\partial_+\chi \\ J_- &= (\rho_1+\rho_2)\,\partial_-\chi \\ J_0 &= \omega \end{aligned}$$

The $2D$ plasma in strong magnetic field

This is probably described by the equation

$$\Delta\psi + \frac{1}{2}\sinh(\psi)\left[\cosh(\psi) - 1\right] = 0 \tag{2}$$

(see however the Second Part for a certain ambiguity in the application of the Bogomolnyi procedure, originating from the absence of a topological constraint on the residual energy term. This is due to the triviality of the first homotopy group of the manifold of the $su(2)$ algebra).

Numerical solution for $L = 307$: monopolar vortex

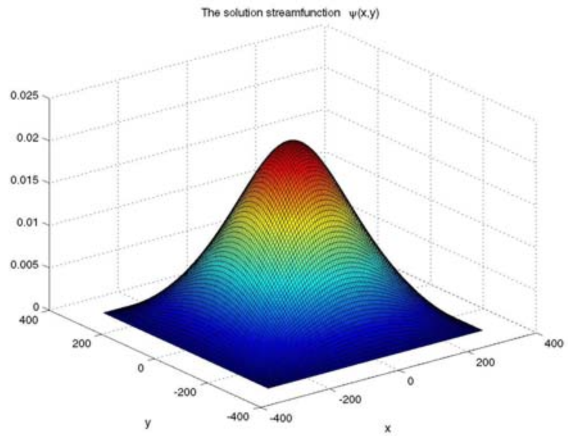

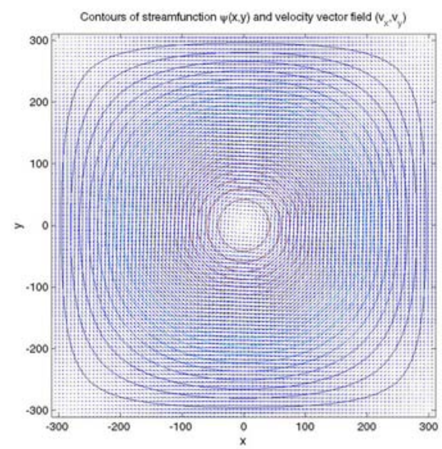

Figure 3: The streamfunction (φ/B) and the velocity, $v_\theta(x,y)$

Physical parameters: $\rho_s = 0.003 \ (m)$, $L^{phys} = a = 1 \ (m)$

After normalization $L = \frac{a}{\rho_s} = \frac{1}{0.003} \simeq 330$

The unit of velocity is $c_s = 9.79 \times 10^3 \sqrt{T_e\,(eV)} \ (m/s)$

Numerical solution for $L = 307$: dipolar vortex

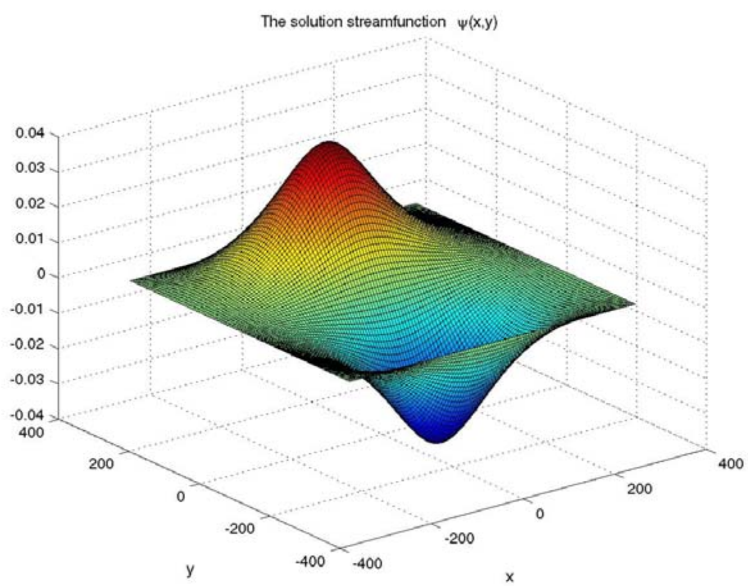

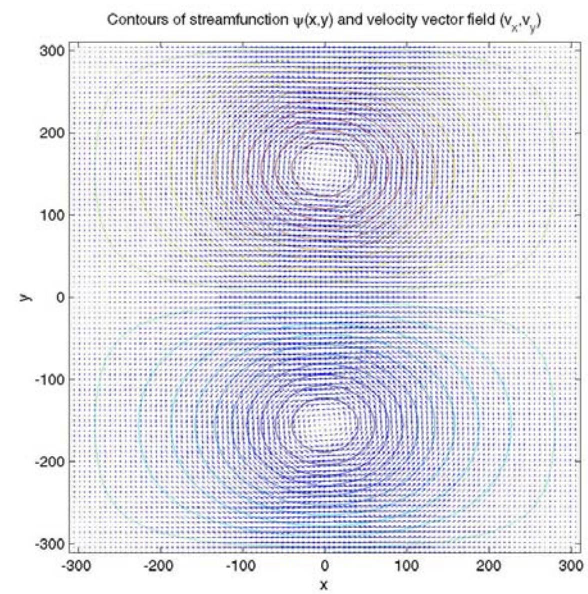

Figure 4: The streamfunction (φ/B) and the velocity, $v_\theta(x,y)$

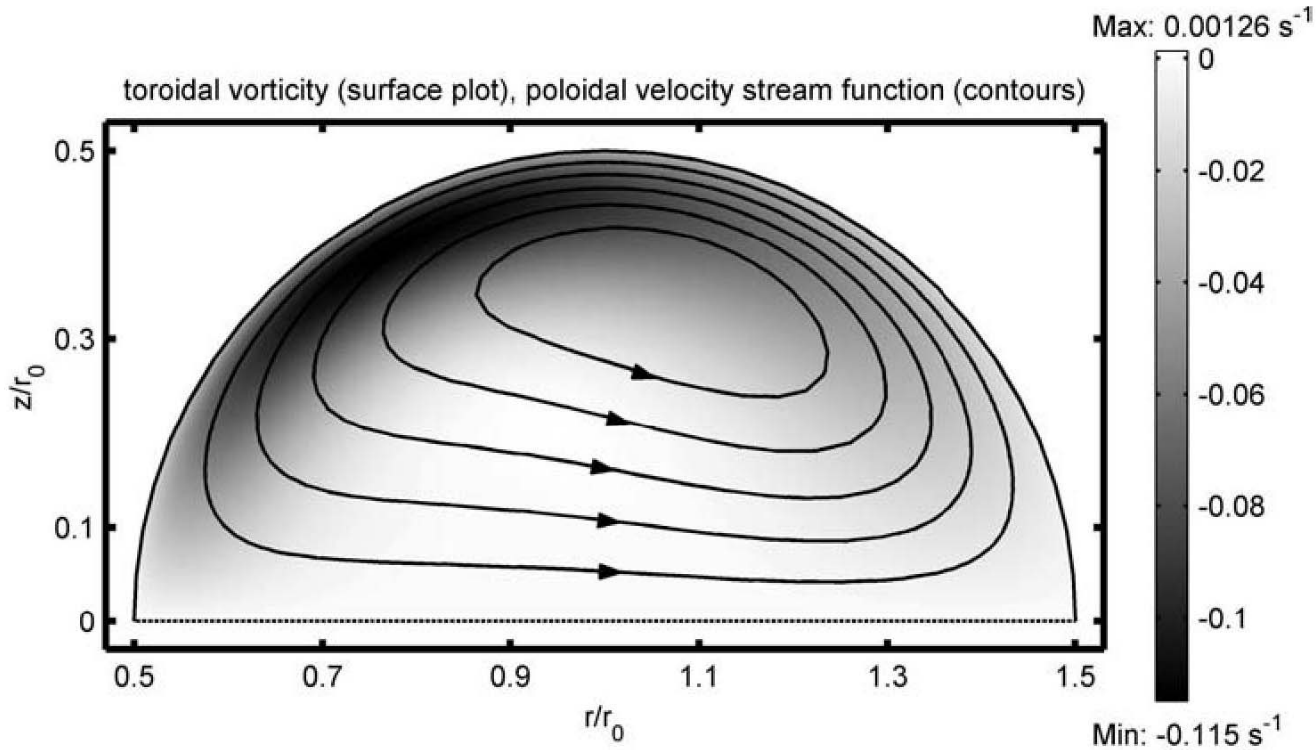

Figure 5. Surface plot of the (dimensional) toroidal vorticity ω_φ combined with contours of the poloidal velocity stream function ψ with M $= 8.64 \times 10^{-5}$. The grey–scale bar indicates the dimensional value of the toroidal vorticity in s^{-1}. Stress–free boundary conditions are assumed.

Figure 5: The streamlines obtained from a direct numerical simulation by Kempe and Montgomery.

Numerical solution for $L = 307$: quadrupolar vortex

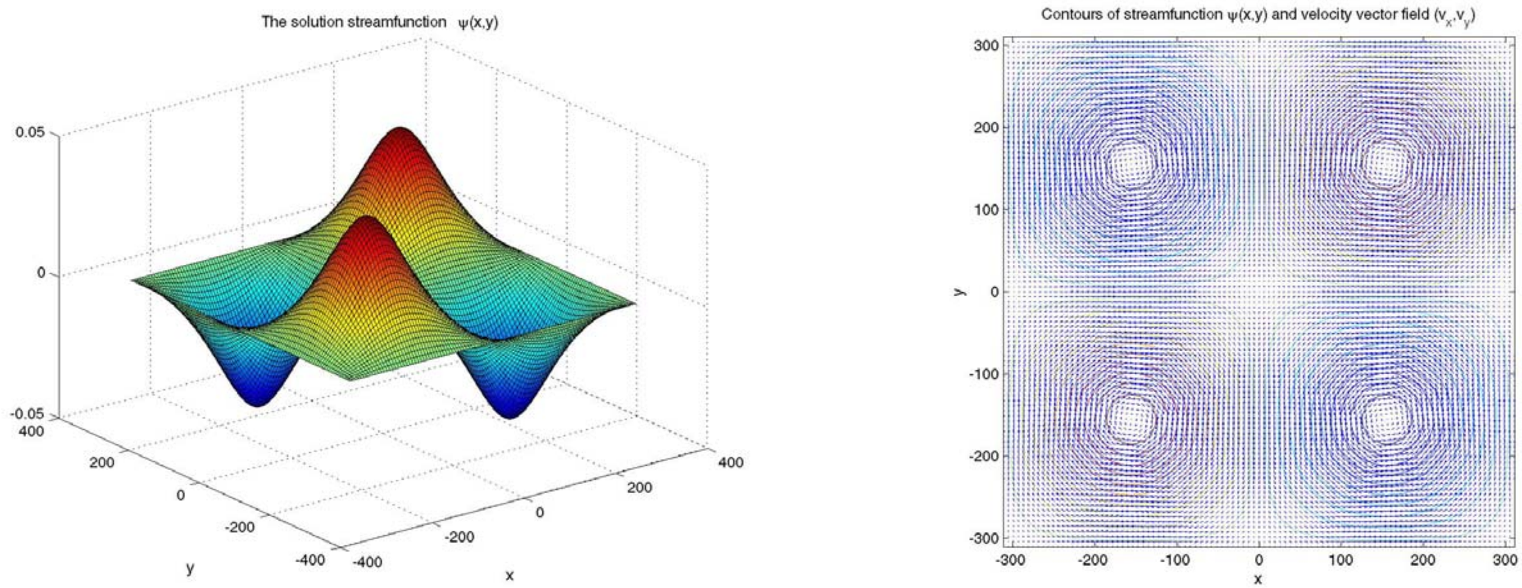

Figure 6: The streamfunction (φ/B) and the velocity, $v_\theta(x,y)$

The multipolar solutions are accessible from a subset of initial conditions.

Self-organisation of the drift turbulence (Wakatani-Hasegawa)

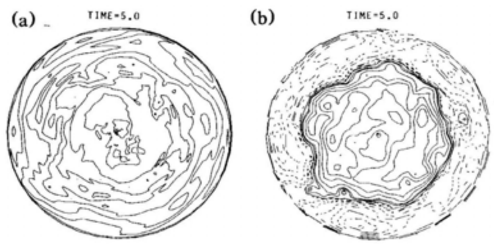

FIG. 1. (a) The density contour and (b) the potential contour from the three-dimensional computer simulation of electrostatic plasma turbulence in a cylindrical plasma with magnetic curvature and shear. In (b) the solid (dashed) lines are for the positive (negative) potential contours. Note the development of closed potential contours near the $\phi \simeq 0$ surface.

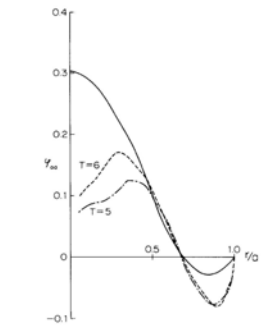

FIG. 2. Profiles of $\phi(r)$ for $m=0, n=0$ mode at two different time steps (dashed and dash-dotted lines) as compared with the predicted profile (solid line) based on the self-organization conjecture. The predicted curve is fitted at $r/a=0.5$.

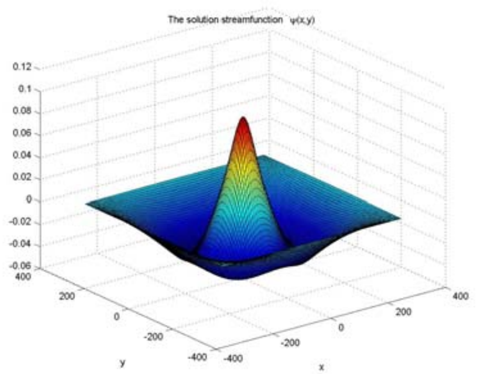

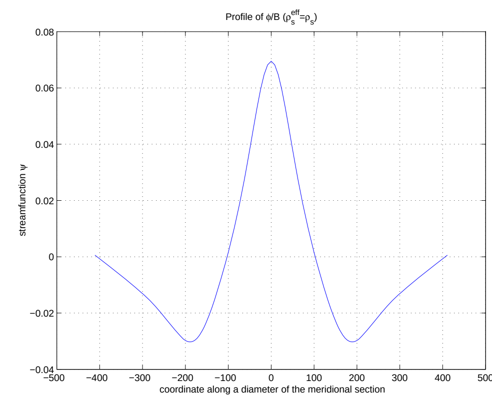

The LH transition

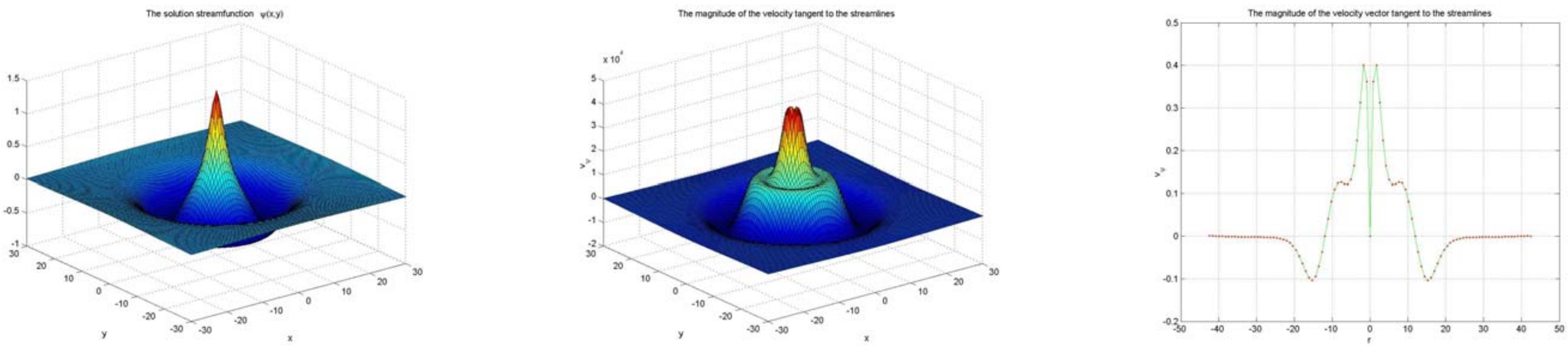

Figure 7: Density series30, set_1.02. $p = 1$ and $L = 30$. Here $ampuh = 1.02$. The streamfunction $\psi(x,y)$ (f53), the azimuthal velocity $v_\theta(x,y)$ (f54) and $v_\theta diag$ (f55).

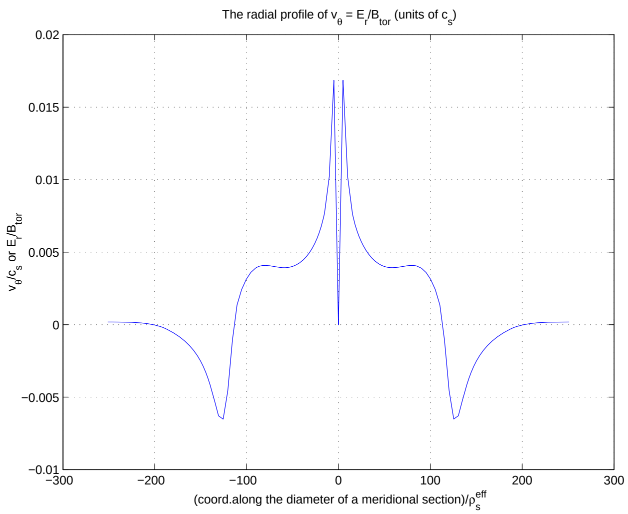

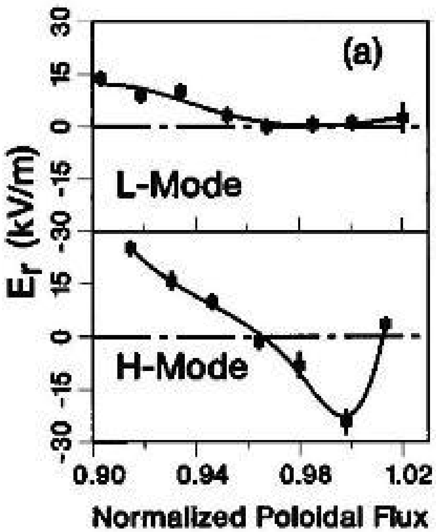

Figure 8: Profile of the radial electric field obtained as a stationary state from Eq.(1) and an experimental obs. DIII-D (Burrell, 1997).

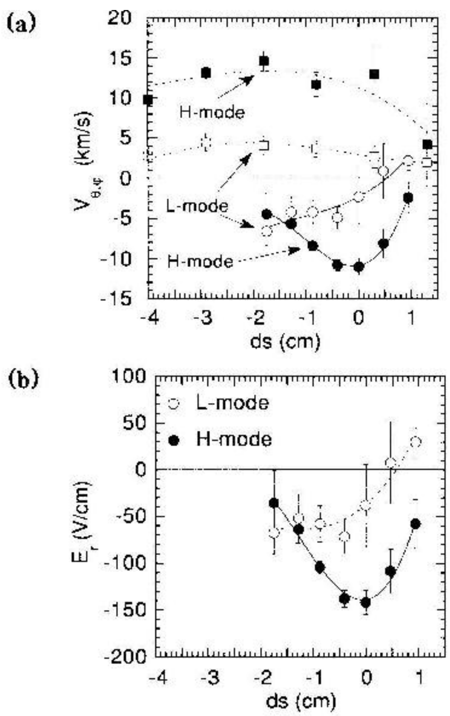

FIG. 3. Radial profiles of (a) poloidal (circles) and toroidal (squares) rotation velocities and (b) radial electric field, as a function of the distance from the separatrix, for *L*-mode ($t=710$ ms, open symbols) and *H*-mode ($t=740$ ms, closed symbols) plasmas. d_s is negative inside and positive outside of the separatrix.

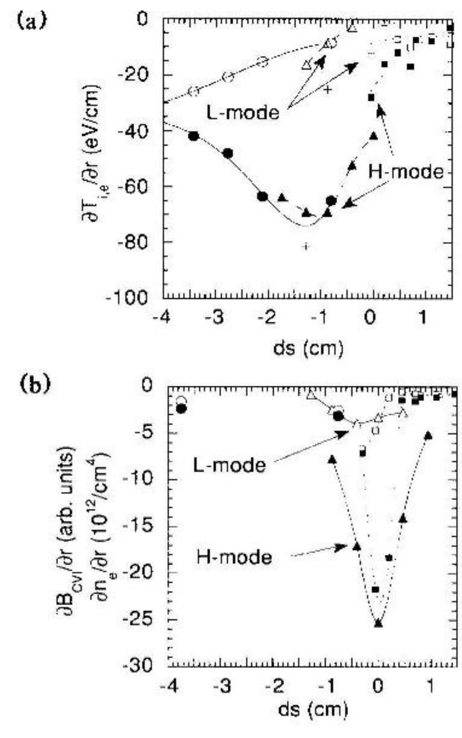

FIG. 4. Gradients of (a) electron temperature measured with ECE radiometer (circles) and electric probes (squares) and ion temperature (plusses for $t=740$ ms, triangles for $t=760$ ms), and (b) electron density measured with Thomson scattering (circles) and electric probes (squares) and brightness of C VI emission (triangles), as a function of the distance from the separatrix for *L*-mode ($t=710$ ms, open symbols) and *H*-mode ($t=740$ ms, closed symbols) plasmas.

Figure 9: Experiments on JET: the poloidal rotation velocity has the same order of magnitude as the diamagnetic velocity

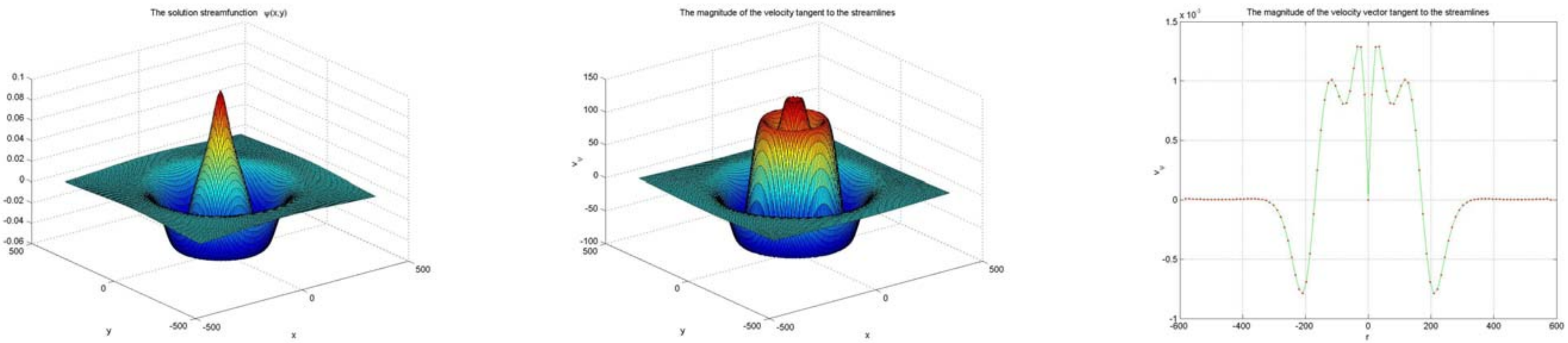

Figure 10: LH structure, $L = 411$. streamfunction and v_θ.

The radial electric field at the edge (H mode)

The value is dependent on the effective Larmor radius, ρ_s^{eff}.

v_d/u	ρ_s^{eff}/ρ_s	$L = a/\rho_s^{eff}$	$\|v_{\theta bottom}\|$	$\left\|v_{\theta bottom}^{phys}\right\| (m/s)$	$\|E_r\| (kV/m)$
0.2	1.118	273	1×10^{-3}	979	2.45
0.4	1.29	236	1×10^{-3}	979	2.45
0.85	2.58	95	2.2×10^{-3}	2152	5.38
0.95	4.47	63	0.02	19580	48.95

The concentration of vorticity

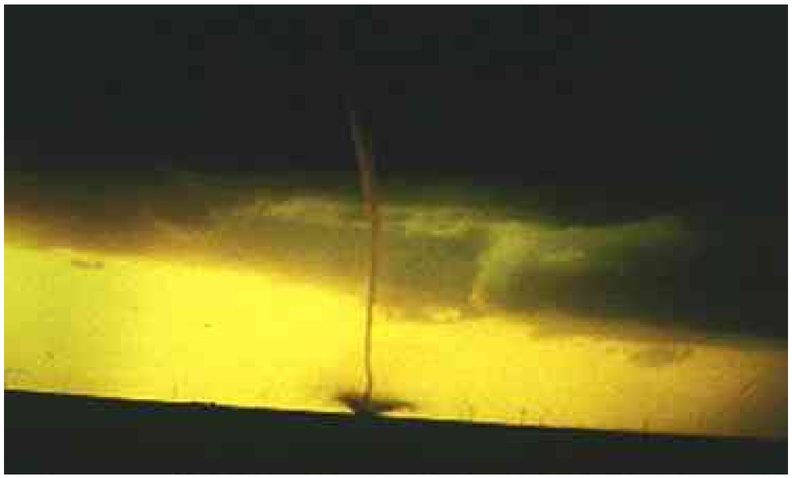

Tornado vortex.

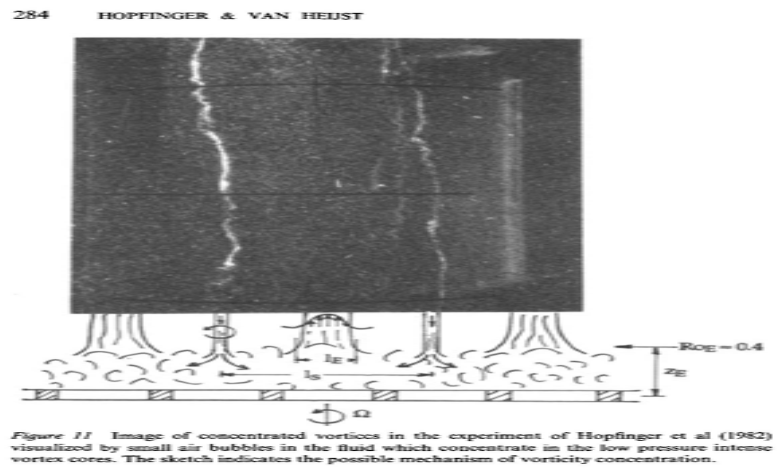

Concentration of vorticity in fluids.

What makes the vorticity which is initially spread in the volume to get concentrated into such narrow, almost string-like, vortices? The answer may be that lower energy states are accessed in this way.

The pinch of density

There can be in FT two processes leading to density pinch:

- the adiabatic evolution of the solutions of the quasi-self-dual states due to the additional energy (which is not topological); we still have to prove that the evolution is toward concentrated filaments.
- the combined effect of the density and vorticity profiles, mediated by the effective Larmor radius.

The role of the effective Larmor radius ρ_s^{eff}

In **Stationary vortices drift waves Nycander** it is derived the equation

$$\Delta\phi = \left(\frac{1}{u}\frac{n_0'}{n_0} + \frac{1}{\tau(x)}\right)\phi$$

where $\tau(x) \equiv \frac{T_e(x)}{T_0}$ and the normalizations are usual: ρ_s , Ω_i and

e/T_e for space, time, potential. Taking constant temperature

$$\begin{aligned}
\frac{1}{u}\frac{n_0'}{n_0}+\frac{1}{\tau(x)} &= \frac{1}{u^{phys}\left(\frac{\Omega_i}{\rho_s}\right)}\frac{1}{n_0}\frac{dn_0}{dr^{phys}/\rho_s}+1 \\
&= 1+\frac{c_s\rho_s}{\Omega_i}\frac{1}{L_n}\frac{1}{u} \\
&= 1-\frac{v_d}{u}
\end{aligned}$$

where $v_d \equiv -\frac{c_s\rho_s}{\Omega_i}\frac{1}{L_n}$ such that when $L_n<0$ we have $v_d>0$

Our model consists of point-like vortices (in their FT *avatar*).

There is a new factor: the density $n(\mathbf{r},t)$.

A positive feedback loop for density pinch

Comparing the Taylor model with the FT model, we find

$$|\kappa| = \frac{16\pi e^2}{J_0^2 a^2 c} \frac{1}{T_m/T_m^c - 1}$$

from which we see that a very peaked current profile in the form of a concentrated filament, *i.e.*

$$T_m \rightarrow T_m^c$$

corresponds in field theory to very high values of κ.

In the statistical model we cannot find an intrinsic reason for T_m to approach (from above) the critical value T_m^c. In FT we ask when there can be reasons for κ to increase adiabatically its value.

In FT, where $\kappa \equiv c_s = \rho_s \Omega_{ci}$ we can assume that κ behaves as ρ_s. An increase of κ can result from an increase in ρ_s.

The spatial variation of the density (*i.e.* $L_n \neq \infty$) is the cause for the diamagnetic flow with the velocity $v_{dia} = \rho_s c_s / L_n$. The distance of interaction between two elementary vortices is modified, replacing ρ_s with ρ_s^{eff},

$$\frac{1}{\left(\rho_s^{eff}\right)^2} = \frac{1}{\rho_s^2}\left(1 - \frac{v_{dia}}{u}\right)$$

- gradient of density increases, L_n is smaller, v_{dia} increases;
- the factor $(1 - v_{dia}/u)$ decreases, ρ_s^{eff} increases;
- the parameter κ increases (since proportional with ρ_s^{eff});
- the increase of κ is equivalent to $T_m \searrow T_m^c$, we find that there is an enhanced clusterization of the elements of vorticity, with a possible evolution toward a single filament in the center.

An intrinsic saturation of density pinch

When the effective Larmor radius is too big, the interaction between the elements of vorticity is no more of short range but can be considered of long range. Or, this is the case of the Euler fluid, where the range of interaction is Coulombian ($i.e.$ ln). For the Euler fluid there is no compressibility of the background density, the density and the vorticity are decoupled and the density cannot follow the vorticity. The compressibility of the ion polarization drift is proportional with the *inverse* of the square of the effective Larmor radius and this diminishes accordingly.

The tropical cyclone

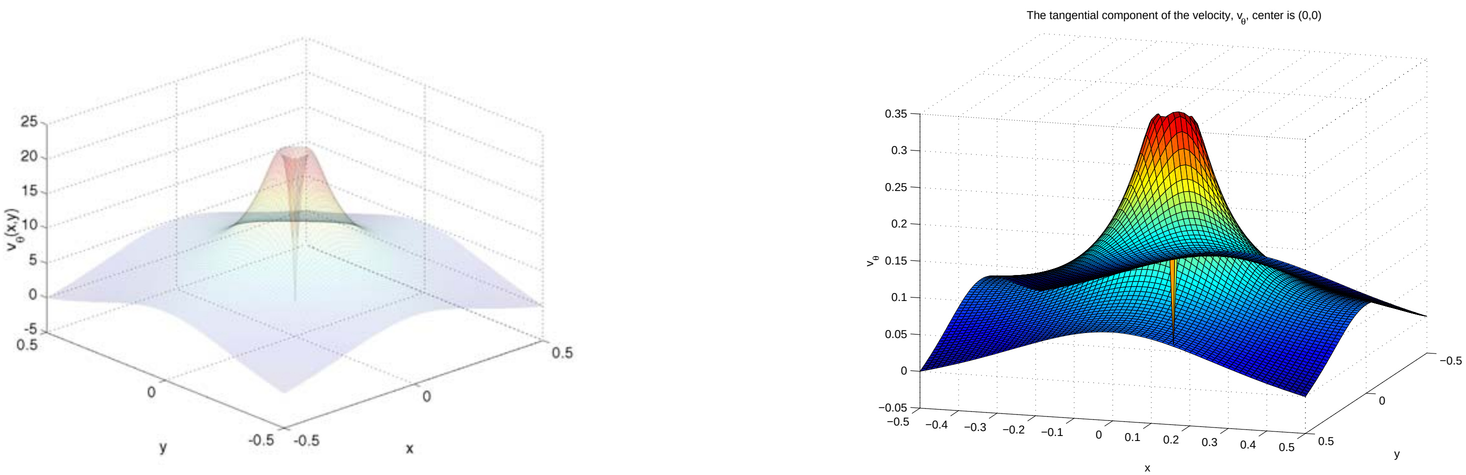

Figure 11: The tangential component of the velocity, $v_\theta(x, y)$

This is an atmospheric vortex.

The tropical cyclone , comparisons

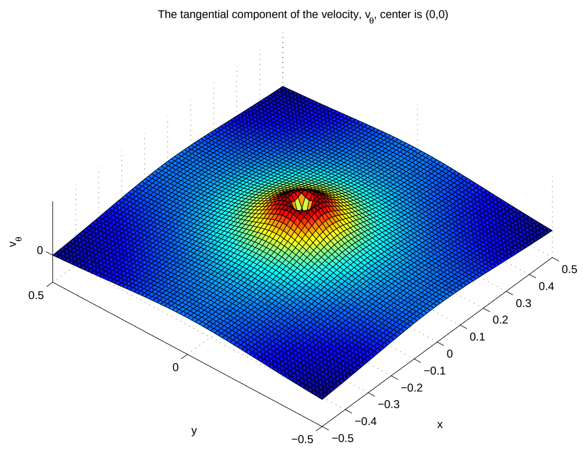

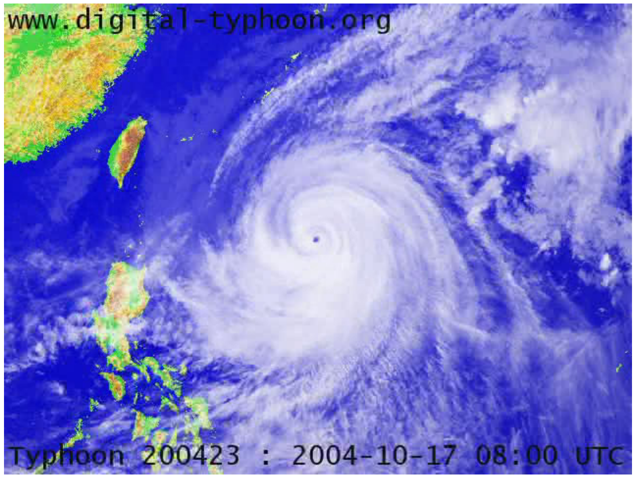

Figure 12: The solution and the image from a satelite.

The solution reproduces the *eye* radius, the radial extension and the vorticity magnitude.

Scaling relationships between main parameters of the tropical cyclone eye-wall radius, maximum tangential wind, maximum radial extension

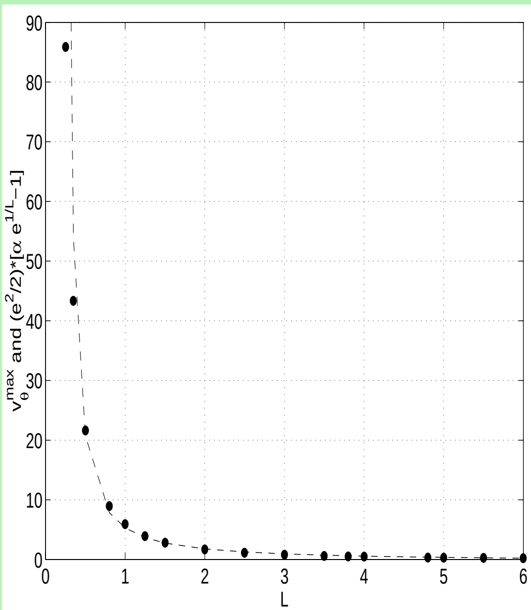

$$v_\theta^{\max}(L) \simeq \frac{e^2}{2}\left[\alpha \exp\left(\frac{\sqrt{2}}{R_{\max}}\right) - 1\right]$$

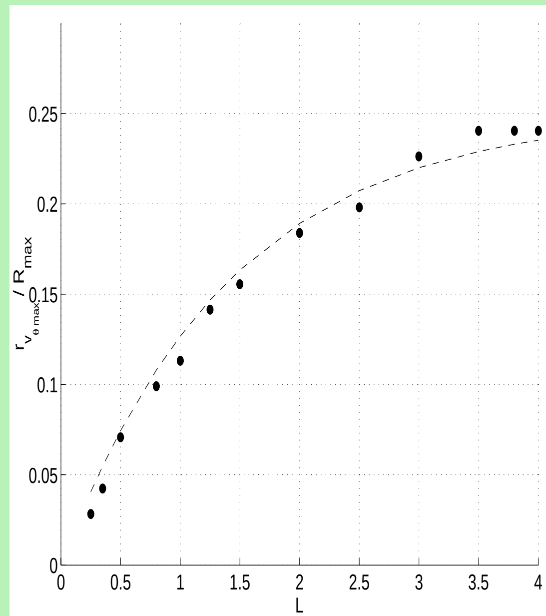

$$\frac{r_{v_\theta^{max}}}{R_{max}} = \frac{1}{4}\left[1 - \exp\left(-\frac{R_{max}}{2}\right)\right]$$

Profile of the azimuthal wind velocity $v_\theta(r)$

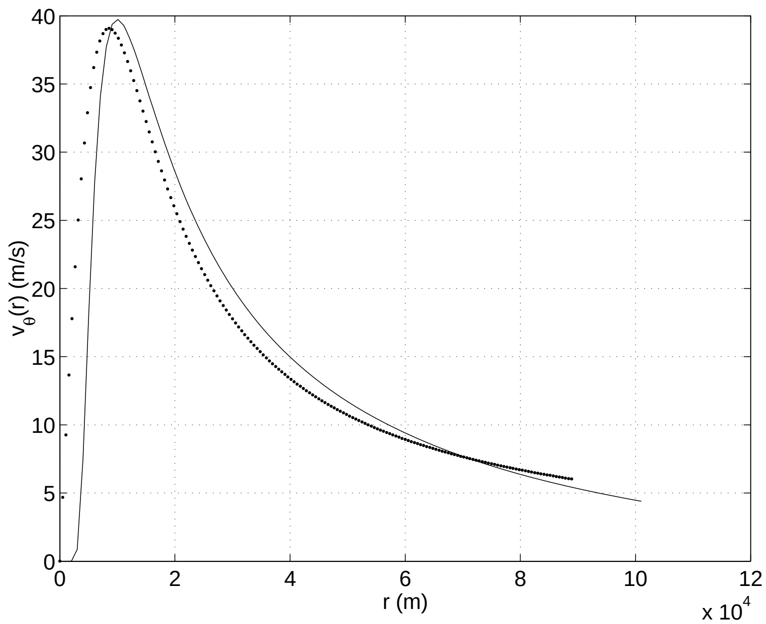

Comparison between the Holland's empirical model for v_θ (continuous line) and our result (dotted line).